Volume 6 Issue 2 (2018) 145-161 ISSN 2347 - 3258
International Journal of Advance Research and Innovation

Design, Development and Fabrication of a Go-Kart

PK Jain[1], Pankaj Yadav [1], Aditya Natu[2], Mukesh Kumar Mandal[2], Parikshit Garg[1], Geetanshu Ashpilya[1], Ashutosh Panpalia[1], Deept Madhav[3], Kunal Mathur[1]
[1]Department of Mechanical Engineering, Delhi Technological University, New Delhi-110042, India
[2] Department of Production and Industrial Engineering, Delhi Technological University, Delhi, India
3Department of Automobile Engineering, Delhi Technological University, Delhi, India

Article Info
Article history:
Received 24 January 2018
Received in revised form
10 March 2018
Accepted 20 May 2018
Available online 15 June 2018

Keywords- Go-Kart, ANSYS Workbench, Catia, Solidworks, FEA

Abstract
Go-Karts are widely used across the world for recreational or professional racing purposes. The following paper includes the whole designing methodology of the various components of a go-kart, designed and manufactured by students of Delhi Technological University. The go-kart was designed conforming with standard principles and considering all major factors and parameters for design and simulation, developing a fully failure analyzed ergonomic go-kart, powered by an internal combustion engine of capacity 125cc. Detailed calculations were done for all the components and 3-d modelling and simulation were performed on professional softwares. The go-kart was fabricated following the industrial norms

1. Introduction

The main objective behind this effort was to design and manufacture a fully functional racing Go-Kart according to industrial parameters that will perform as per expectations and the standards set by the industry, and in the process enhance our technical skills. The aspects of ergonomics, safety, ease of manufacture and reliability are taken into consideration while designing. Incorporating standard design methodology enabled us to achieve an optimum design. This project provides an opportunity to students like us having ample theoretical knowledge of engineering concepts, to get familiar with the challenges faced during the actual designing and manufacturing phases of real life products, which are very crucial for a practicing engineer.

The initial design of the chassis was made in Solidworks 2016 considering the ease of manufacturability and a proper methodology was followed for production which enabled us to manufacture the Go-Kart at a faster and efficient way. Many parameters were optimized by using higher grade material which weighed less, and ANSYS 18.1 with the feature of topology optimization also played a crucial role. The use of CATIA V5 R20 for making the chassis more ergonomic, hence improving on the driver comfort and performance, as well as the kart performance.

2.Literature Review

The research field in the domain of automobile chassis has evolved a lot with time and progress has been made according to the type of utility of a specific vehicle. Most of the research papers on chassis design focus on factors like proper handling of a variety of loads and perform crash tests for driver safety assurance [1][13] without analyzing the ergonomic aspects. [21] uses finite element techniques to perform analysis on the Go-Kart chassis for stress distribution and deflection but does not include ergonomics and driver comfort. [17] focuses on designing an optimum Ackermann steering geometry using rack and pinion by developing a new mathematical model, but it does not elaborate on design and simulation of real time mechanical components used in the steering assembly, such that the limitations of a particular geometry are highlighted. [19] uses the engine parameters to calculate sprocket dimensions, frictional torque and the factor of safety of the Go-Kart shaft designed, but does not consider the parameters like transmission efficiency that affects the performance of spur gears and chain sprocket assembly and it does not state the maximum corresponding acceleration in each gear.

While designing the Go-Kart chassis, a lot of parameters like driver safety and ergonomics, optimization in weight, rear jacking effect for shock absorption, space for engine cooling have been considered and successfully implemented. Preference of pitman arm over rack and pinion type has been illustrated as well as a comparison graph between the steering angle and the tyre angle was generated using MSCAdams. In addition to steps in [19], maximum acceleration in each gear, load shift calculations, consideration of transmission efficiency and a relation between the tractive force and the kart speed for each gear have been calculated.

***Corresponding Author,**
E-mail-address: pkjain@dce.ac.in

3. Kart Specifications

The kart specifications have been chosen so as to achieve the required performance and maximum output, while also keeping in mind the constraints mentioned in the guidelines. Table 1 summarizes a list of the kart specifications.

Table 1 : Kart Specifications [6]

Dimensional Data	
Wheelbase	1100mm
Track Width	880mm
Ground Clearance	1.25inch
Length/Width/Height	1925.4mm/985.4mm/845.1mm
Kerb Weight	95 kg
Fuel Tank Capacity	5 litres
Performance Data	
Engine	Honda CBF Stunner
Engine Technology	PGM-Fi
Max Torque	11 Nm
Max Power	11.15 HP
Power to Weight Ratio	85.27 bhp/tonnes
Transmission Type	5 speed sequential
No. of Speed Gears	5
Ignition Type	Single Spark
Steering System	
Steering wheel diameter	304.8 mm (12 inch)
Spindle to spindle distance	700 mm
Length of steering arm	115 mm
Steering arm angle	17.65 degree
The rod length	305.41 mm
Maximum steering wheel angle	38.78 degree
Brakes System	
Brake pedal ratio	6:1
Master cylinder piston diameter	0.75 inch
Caliper piston diameter	1 inch
Brake disc diameter	170 mm

3.1. Chassis and Design

3.1.1. Definition and Purpose

The chassis is the central frame of a vehicle which has to carry all the components and support all the loads. These loads include the weight of each component and the forces which manifest during acceleration, deceleration and cornering. [13]

Chassis of a go-kart plays a significant role in the jacking of the kart while the kart is cornering. In the absence of a differential in a kart, chassis frame plays following pivotal roles in the performance [22]:

It allows, lifting of the rear inside wheel of the kart while cornering by the virtue of its flexibility and relatively low torsional stiffness. This can cause the kart to turn very smoothly even without a differential.

It acts as a shock absorber which absorbs various shocks and vibrations from the road to provide maximum comfort to the driver.

3.1.2. Design Objectives

The frame of the kart chassis was designed with following aims [5]:

- To have minimum wheelbase and track-width as permitted by rulebook and ergonomic norms to improve cornering performance
- To weigh less than 15 kg.
- To be flexible enough to allow rear 'jacking' effect and absorb road shocks.
- To protect the driver in front and side crash events.
- To provide comfortable posture to a large range of driver statures.
- To be easy to fabricate.
- To have an open airflow over the engine compartment for cooling.

Keeping the above-mentioned objectives in mind, a *tubular ladder chassis* incorporating features of *space frame chassis* was used to facilitate an open ergonomically suitable compartment. The space frame type is commonly used in race car due to its rigidity and ease of construction. [13]

3.1.3. Design Methodology

Figure 1 shows the design workflow that was adopted for this project.

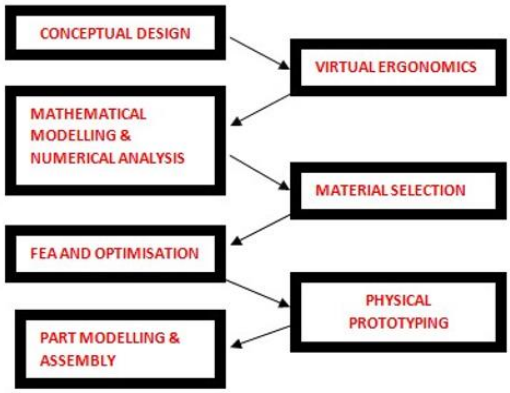

Fig. 1 : Design Methodology

Table 2 : Properties of AISI 1020 [7]

Conceptual design was initially agreed upon keeping all the initial design parameters in view. Thereafter, a virtual model of the go-kart frame was developed using SolidWorks 2016, then static and dynamic simulations were carried out using ANSYS Workbench 12.0. The stress and modal analysis techniques are significantly essential for automotive chassis structure design. It is important to study the dynamic characteristic of the chassis so that resonance and structure failure does not occur on the chassis in working condition. [14].

These softwares greatly reduce the effort and finance required for developing prototypes by providing a platform using which virtual models can be developed and tested.

The model was further analyzed in ANSYS for cornering performance and vibrational analysis etc. and ergonomic analysis was done in CATIA V5 R20. Some changes were made in the design to satisfy all conditions necessary. Multi-body modelling has been performed to accommodate all the other components on the frame.

3.1.4. Chassis Specifications

Material Selection: Various parameters were kept in mind while selecting the frame material which includes availability, cost, machinability and tensile strength. Fig. 2 shows a comparison of the deciding parameters for 3 different materials. After analyzing these 3 materials it was concluded that AISI 1020 will be the material for the chassis due to its following properties:

- Low cost
- High Machinability
- High Availability
- Moderate Strength

Table 3 : Chemical Composition of AISI 1020 [7]

Property	Value
Density	7.87 g/cc
Elastic Modulus	205 GPa
Poisson's Ratio	0.290
Yield Strength	350 MPa
Ultimate Tensile Strength	420 MPa
Thermal conductivity	51.9 W/kg
Coefficient of thermal expansion	11.7 um/m
Brinell hardness	111

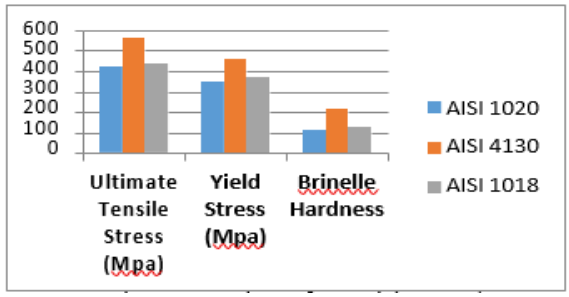

Fig. 2 : Comparison of Material Properties [7]

Table 3 : Chemical Composition of AISI 1020 [7]

Element	Content
Carbon, C	0.17-0.23%
Iron, Fe	99.08 - 99.53 %
Manganese, Mn	0.30 - 0.60 %
Phosphorous, P	≤ 0.040 %
Sulphur, S	≤ 0.050 %

According to American Iron and Steel Institute, following is depicted by 1020:

- The first digit shows that it is plain carbon steel.
- Second digit shows that there are 0 alloying elements.

The last two digits show that the steel contains approximately 0.20% carbon which depicts the best machinability

3.2Cross Section

The cross section for the members was chosen as circular tubular for its higher torsional stiffness for a given area of cross section compared to square and other sections and because of its uniform distribution of stresses resulting in low stress concentrations. The standard cross section determined after market research was 25.4mm outer diameter and 22.4mm inner diameter.

3.3 Equivalence Calculations of Cross Section of Tubes Used :

3.3.1Material AISI 1020

Modulus of Elasticity, E=205 GPa

3.3.2 Case-1

For Outer diameter = 1 inch, Thickness = 1.5 mm

Moment of Inertia, $I = \pi (D^4 - d^4)/64$ [9]= 8073.32 mm^4

Bending stiffness = EI [9]= 205 * 1000 * 8073.32 $N\text{-}mm^2$ = 1655030655 $N\text{-}mm^2$ = 1655.03 $N\text{-}m^2$

Polar Moment of Inertia, $I_p = \pi(D^4 - d^4)/32$ [9]= 16146.64 mm^4

Torsional Stiffness (per unit length) = GI_p [9]= 1291.73 Nm/rad

3.3.3 Case-2

For Outer diameter = 1 inch, Thickness = 1.65 mm

Moment of Inertia, $I = \pi(D^4 - d^4)/64$ = 8722.20 mm^4

Bending Stiffness = EI = 205 * 1000 * 8722.20 $N\text{-}mm^2$ = 1788051264 $N\text{-}mm^2$ = 1788.05 $N\text{-}m^2$

Polar Moment of Inertia, $I_p = \pi(D^4 - d^4)/32$ [9]= 17444.40 mm^4
Torsional Stiffness (per unit length) = GI_p =1395.55 Nm/rad

Table 4 : Bending Stiffness of Different Materials

Material	Bending Stiffness (Nm^2)			
	At D=1 in & t= 1.5mm	At D=1.25 in & t=1.5 mm	At D=1 in & t=1.65 mm	At D= 1.25 in & t=1.65 mm
AISI 1020	1655.03	3350.8	1788.05	3633.29
AISI 4130	1695.4	3432.52	1831.67	1831.67
AISI 1018	1655.03	3350.84	1788.07	3633.29

3.4 Final Chassis Layout

The three normal views of frame are shown in figures 3-6.

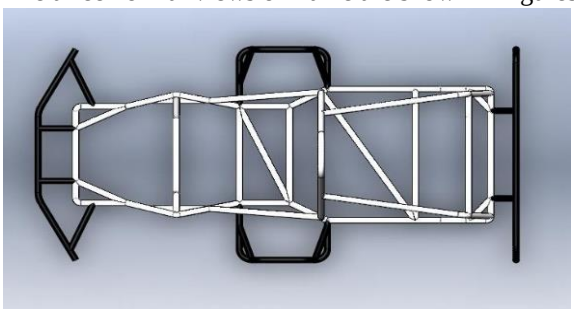

Fig. 3 : Top View of Chassis

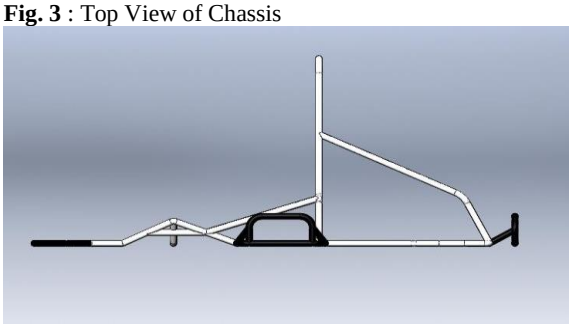

Fig. 4 : Side View of Chassis

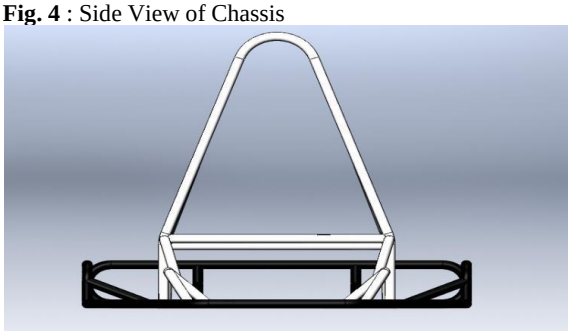

Fig. 5 : Front View of Chassis

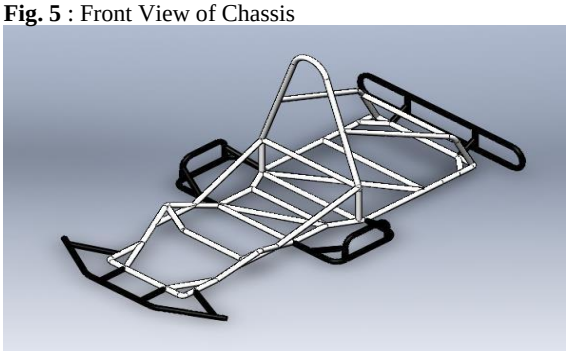

Fig. 6 : Isometric View of Chassis

3.5Final Geometrical Parameters

Major dimensions which associated with the frame have been tabulated in Table 5.

Table 5 : Frame Parameters

Parameter	Value
Wheelbase	1100 mm
Front Track	880 mm
Rear Track	880 mm
Total Length	1925.4 mm
Total Height	845.1 mm
Total Width	985.4 mm
Total Chassis Weight	12.885 kg
Cross Sectional Data	
Type	Tubular
Outer Diameter	25.4 mm
Inner Diameter of Chassis Members	22.4 mm
Inner Diameter of Bumper Members	22.1 mm

3.6. Finite Element Analysis

3.6.1FEA methodology

The finite element theory was employed for predicting the behaviour of chassis under the methods proposed in the Fig.7.

FEA is a method in which the model is divided into small elements, properties of which are then evaluated using general equations of motion and boundary conditions specified during a test. This involves solution of the equation: [2]

[Reaction]=[Stiffness]∗[Displacement]+ [Load]

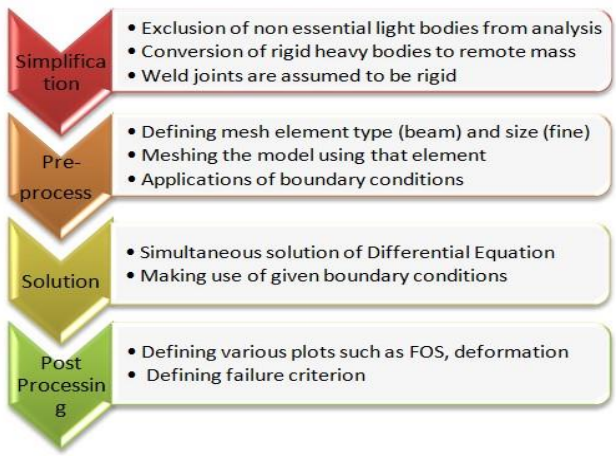

Fig. 7 : Design Methodology [4]

The non-structural elements such as driver and engine were modelled as remote mass acting on their respective mounting positions. Also, the analysis was done in ANSYS Workbench to get better validated results under same loaded conditions.

3.6.2Grid Characteristics

The frame was meshed from beam elements for analysis. In ANSYS Workbench, the model was generated automatically from beam elements with 6 degrees of freedom for every element.

The members which were predicted to be the heaviest loaded were applied 'fine' mesh control to gain better accuracy. The final mesh for ANSYS Workbench is shown in Fig. 8.

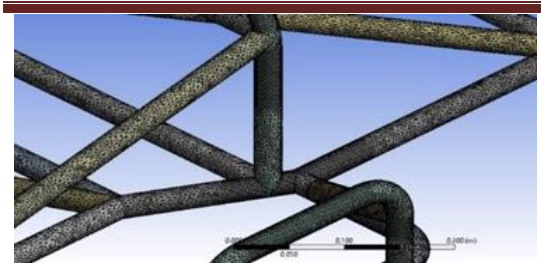

Fig. 8 (a) : Beam mesh in ANSYS Workbench

Fig. 8 (b) : Fine Mesh on the Members

Table 6 : Meshing in Ansys Workbench

Meshing Characteristics	
Physics Preference	Mechanical
Relevance	50
Relevance Center	Fine
Smoothing	Medium
Span Angle Center	Fine
Minimum Edge Length	5.7633e-004 m
Nodes	2242114
Elements	1117384

After setting the mesh, 5 static studies were performed on the model:

a) Static Bending Test
b) Torsional Stiffness Test
c) Front Impact Test
d) Side Impact Test
e) Rear Impact Test

These models have been discussed in detail in the upcoming section.

Loading Diagram Abbreviations: -

- Red Arrows- Driver Weight (600N)
- Red Arrows- Engine Weight (300N)
- Red Arrows- Impact Forces (N)
- Blue Tags- Fixed Supports
- Yellow Arrows- Gravity (m/s^2)

(a) Static Bending Test: In this test, various stresses developed in a fully loaded chassis were analysed.

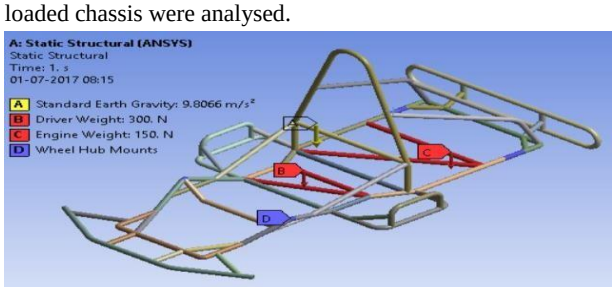

Fig.9 (a) : Loading Diagram

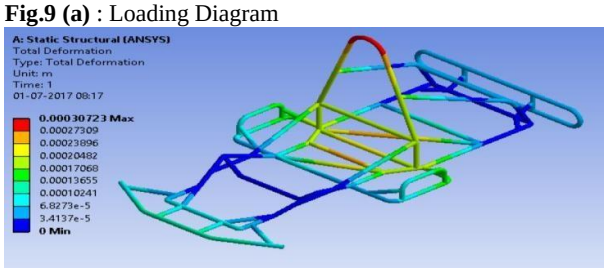

Fig.9 (b) : Total Deformation

Fig.9 (c) Equivalent Stress

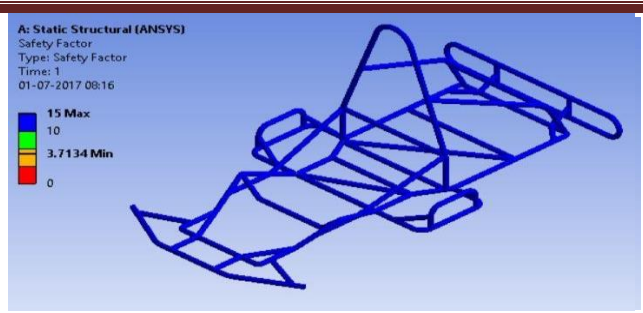

Fig.9 (d) Factor of Safety

Fig. 9 : Results of Static Bending Test

It can be seen from the chart, maximum deformation in base member is 0.27 mm at driver seat during sagging which is acceptable. The highest combined stress was encountered at the side bumpers and its value was 129.5MPa.

The yield stress of AISI 1020 is 350MPa.

$FOS = \frac{Yield\ Stress}{Max\ Combined\ Stress} = 3.71$ [9]

So, the minimum FOS evaluated is 3.71 which is safe against an industrial reference value of 1.5. So, our design is validated for static bending.

(b) Torsional Stiffness test: This test determines the resistance offered by the chassis frame against a twist which is normally developed during cornering, or when the vehicle encounters a bump in the road.

Table 7 : Boundary Conditions

Loads	Driver, Engine, and Gravity loads at mounting positions. A couple of 6035N is applied on the Rear Wheel Hub Mount positions of
Constraints	Front Wheel Hub mounting positions
Gravity	On

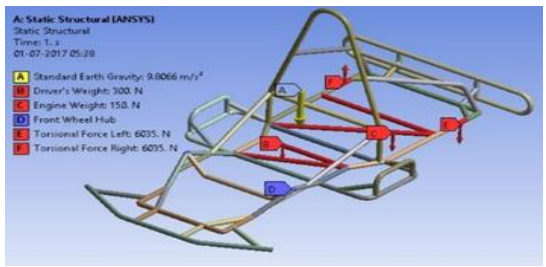

Fig.10 (a) : Loading Diagram

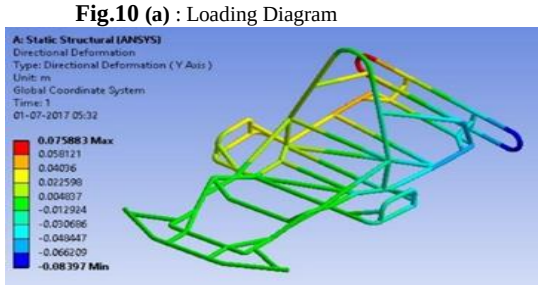

Fig.10 (b): Directional Deformation

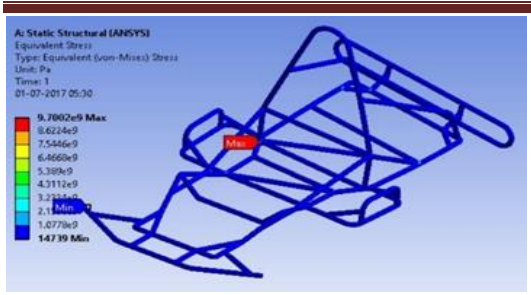

Fig.10 (c): Equivalent Stress

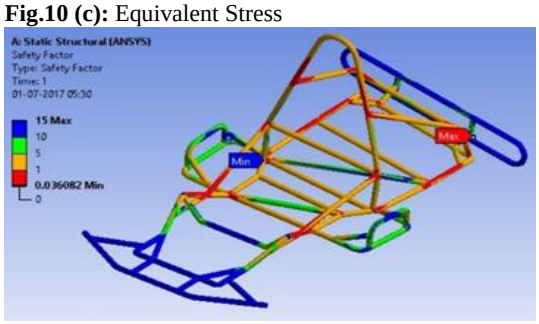

Fig.10 (d): Factor of Safety

Fig. 10 : Results of Torsional Rigidity Test

Directional Deformations at the Rear Wheel Hub Mount positions are 44 mm and 54 mm.

Twist = $\tan^{-1}\left(\frac{D_1 + D_2}{L}\right) = \tan^{-1} 0.1633 = 9.276°$

Torque = 3621 Nm

Torsional Rigidity = Torque⁄Twist

= 3621⁄9.276 = 390.36 Nm/deg

Since this value lies within the standards adopted, it is acceptable.

(c) Front Impact test: This test determines the effect of a crash on the chassis at speeds up to 70 km/h (determined to be the maximum speed when brakes are applied at least for 0.5 seconds before crash).

The collision time in a chassis without a crumple zone is statically averaged to 150ms. But the chassis of this go kart has a mild steel bumper and a thin deformable tube which can act as a crumple zone and increase the collision time to 200ms.

$F = m*(\Delta v/\Delta t)*0.5 = 150 * 70/0.2 * 5/18 *1/2$

F = 7.29 kN

In terms of G, F = 4.955G

Table 8 : Boundary Conditions

Loads	7.29kN applied on front bumper members
Constraints	Front and Rear Wheel Hub Mount Positions
Gravity	On

The FOS of the front cross members amounts to 3, which indicates that they will not fail during collision. However, the FOS in the cockpit has a minimum value of 15, which is safe enough.

Our model can be said to be validated against front impact test at a speed of up to 70 km/h against an industrial reference value of 1.5.

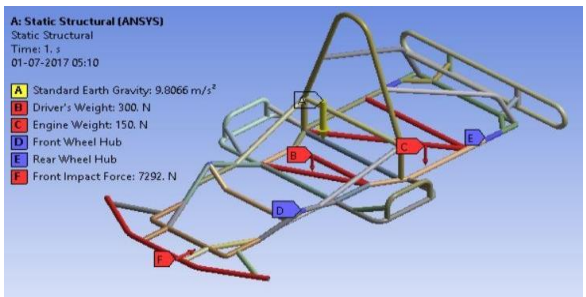

Fig.11 (a): Loading Diagram

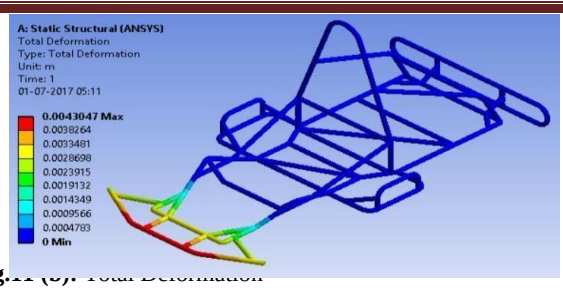

Fig.11 (b): Total Deformation

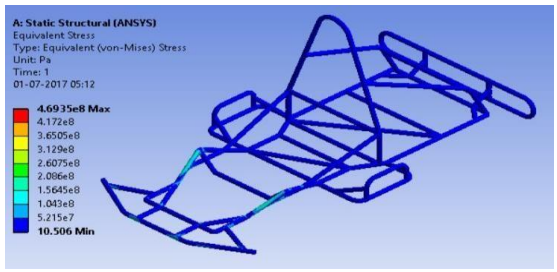

Fig.11 (c): Equivalent Stress

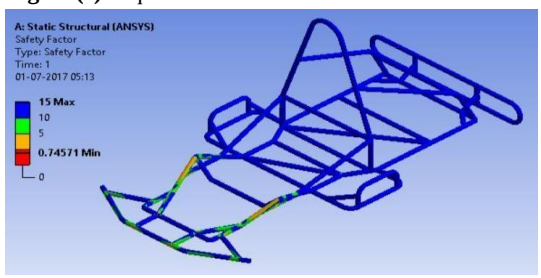

Fig.11 (d): Factor of Safety

Fig. 11: Results of Front Impact Test

(d) Side Impact test: This test determines the effect of a crash on the chassis when another kart collides with it on the side members at an angle of 90°. The maximum speed difference between the karts in such a collision is taken to be 80 km/hr.

$F = m*(\Delta v/\Delta t)*0.5 = 150*(22.22/0.2)*0.5$

F = 8.33 kN, In terms of G, F = 5.66 G

Table 9 : Boundary Conditions

Loads	8.33kN applied on side bumper members
Constraints	Front and Rear Wheel Hub Mount
Gravity	On

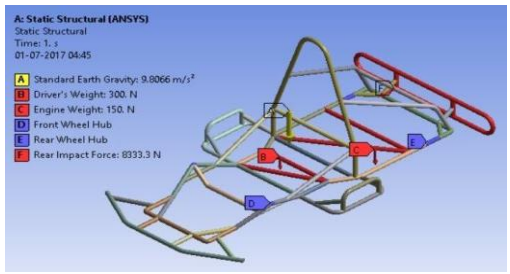

Fig.12 (a): Loading Diagram

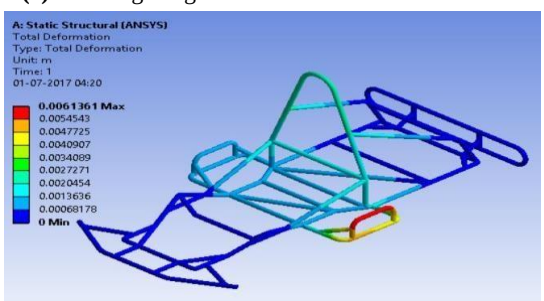

Fig.12 (b): Total Deformation

Fig.12 (c): Equivalent Stress

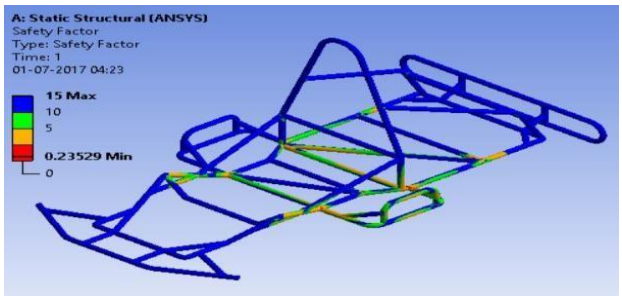

Fig.12 (d): Factor of Safety

Fig. 12 : Results of Side Impact Test

The FOS of the cockpit amounts to 5 which indicates that they will not fail during collision. Our model can be said to be validated against side impact test at a speed difference of up to 80 km/hr against an industrial reference value of 1.5.

(e) Rear Impact test: This test determines the effect of a crash on the chassis when another kart collides with it on the rear members. The maximum speed difference between the karts in such a collision is taken to be 80 km/hr.

$F = m * (\Delta v/\Delta t)*1/2 = 150 * 22.22/0.2 = 8.33$ kN

In terms of G, F= 5.66G.

Table 10 : Boundary Conditions

Loads	8.33 kN applied on side bumper members
Constraints	Front and Rear Wheel Hub Mount Positions
Gravity	On

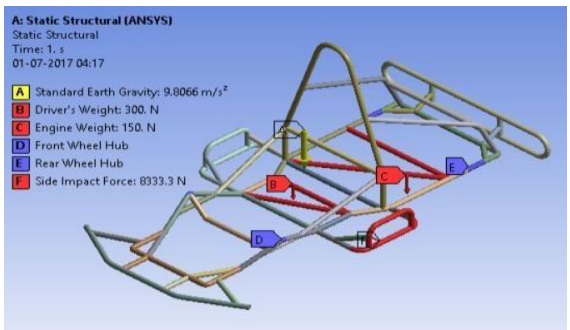

Fig.13 (a): Loading Diagram

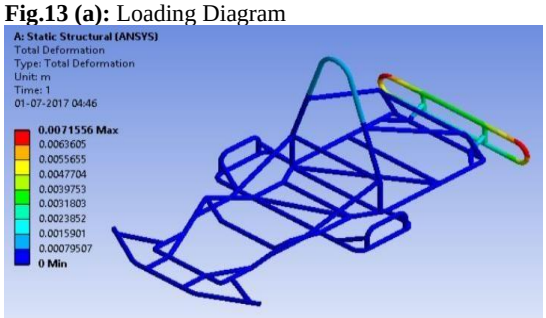

Fig.13 (b): Total Deformation

Fig.13 (c): Equivalent Stress

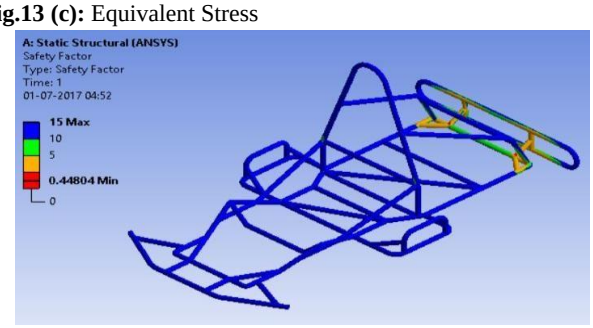

Fig.13 (d): Factor of Safety

Fig. 13 : Results of Rear Impact Test

The FOS of the cockpit amounts to 15 which indicates that they will not fail during collision. Our model can be said to be validated against side impact test at a speed difference of up to 80 km/hr against an industrial reference value of 1.5.

F. Modal Analysis

The global vibrational characteristic of a vehicle is related to both its stiffness and mass distribution. The frequencies of the global bending and torsional vibration modes are commonly used as benchmarks for vehicle structural performance. Bending and torsion stiffness influence the vibrational behavior of the structure, particularly its first natural frequency [16].

This study utilizes modal analysis to generate the natural frequencies and mode shapes of the chassis structure. If any of the excitation frequencies coincides with the natural frequencies of the chassis, then resonance phenomenon occurs. The chassis will undergo dangerously large oscillations, which may lead to excessive deflection and failure. The vibration of the chassis will also cause high stress concentrations at certain locations, fatigue of the structure, loosening of mechanical joints, creation of noise and vehicle discomfort [15]. Result from Modal Analysis is important as it can also predict the response of structural parameters under dynamic loading condition. Mode shapes simulated from Modal Analysis can provide the information of how the chassis structure will naturally displace. ANSYS Workbench Mechanical is used as pre-processor, solver and post-processor for the modal analysis [4]. The mode shapes are extracted using Block Lanczos method. Block Lanczos method has been used in studies for extracting mode shapes and natural frequencies.

Table 11 : Frequencies and Deformations at each modes

Mode	Frequency	Maximum Deformation
1	47.048	0.88484m
2	55.138	0.77644m
3	69.569	0.85726m
4	77.261	1.3113m
5	88.132	0.94202m
6	94.939	0.66217m
7	107.76	0.76488m
8	115.12	1.1874m
9	125.01	0.77368m
10	141.79	0.66935m

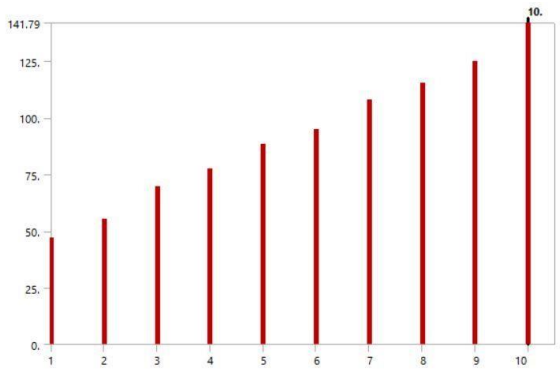

Fig. 14 : Natural Frequencies of Chassis

The analysis found that the natural frequencies extracted using Block Lanczos Method produced 10 mode shapes within 40-150 Hz frequency range. All mode shapes produced natural frequencies which is not coinciding with the primary imbalance frequency 166.66 Hzor secondary imbalance frequency 333.33Hz of engine, which is safe and comfortable. Thus, no resonance will occur, and design is hence validated.

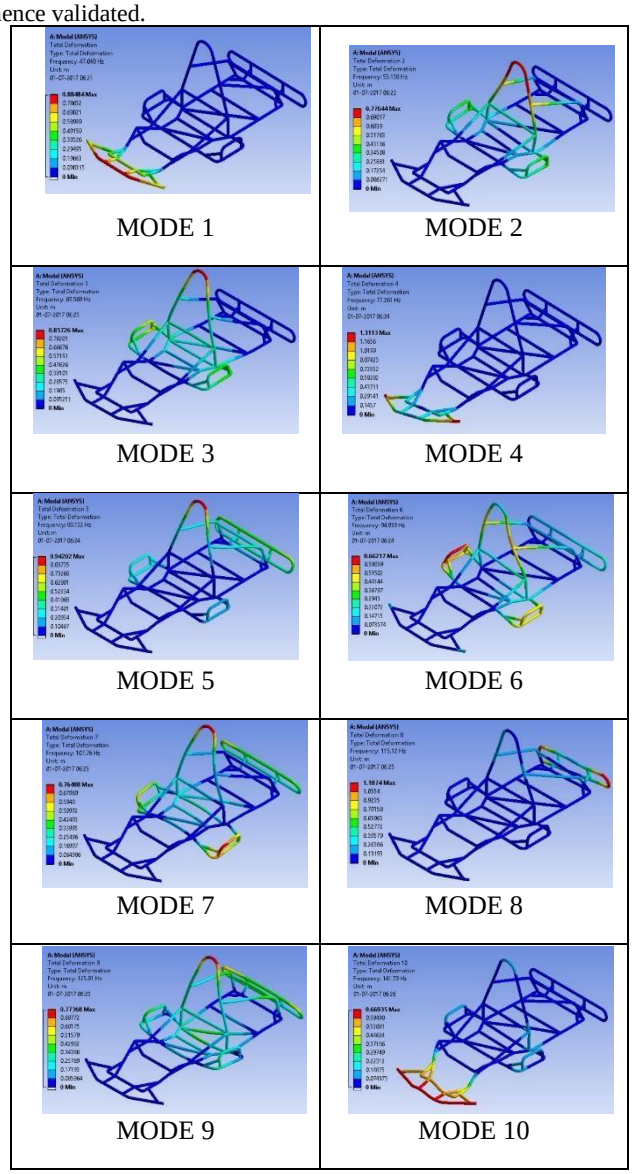

Fig. 15 : Deformation Plots at Different Frequencies

G. Ergonomics

(a) Purpose

Ergonomics is the study of designing equipment and devices that fit the human body and its cognitive abilities. In this project the design of the go kart should be such that all its controls should be comfortably in the reach of the driver's upper body [4].

Also, the vision of the driver should be unobstructed by any part of the go kart as in a dynamic event, vision plays a key role in the driver's and ultimately kart's performance.

(b) Methodology

Ergonomic analysis for the kart was performed in CATIA V5 R20 using its Human Builder and Human Activity Analysis workspaces. The test model or the manikin was first selected on the basis of the stature of the driver. Details are given in Table 12.

Table 12 : Manikin Properties

Property	Value
Population	Korean
Stature Percentile	90
Weight Percentile	6.4
Height	1780 mm
Weight	55 kg
Posture	Custom
CG Height from Ground	170 mm

The manikin was then positioned into the Kart using I-K behaviours and posture-editing.

The Fig. 16 shows the manikin model positioned in the kart, which shows that the knees should be bended outwards for maximum comfort. The red dot represents the C.G. of the driver.

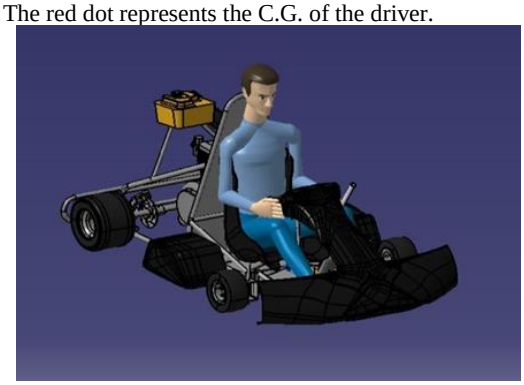

Fig. 16 : Ergonomic Model Isometric

The Fig. 17 shows the peripheral vision contours from the driver's point of view in binocular vision mode. The clear area in the middle represents good focus while the blurred region represents unfocussed vision range. The solid red contour shows the blind spots of the driver without moving.

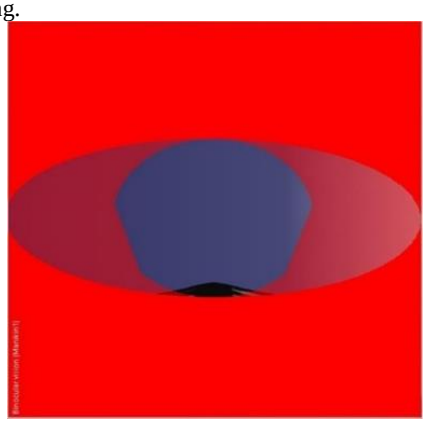

Fig. 17 : Field of Vision

Next an upper limb movement test was performed on the test model to evaluate the reaction performance of the driver in the current

posture setting. This test is known as RULA (Rapid Upper Limb Assessment).
The driver model was evaluated by RULA and an average score of 3 was given.
This score category shows that the driver does have a fine reflex action. However, this score may be attributed to correct posture application in the model.

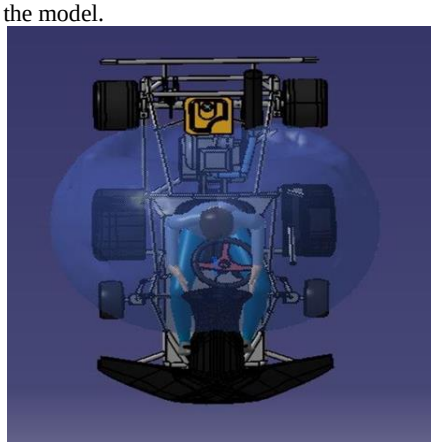

Fig. 18 : Reach Envelope

The above figure shows the reach of the hands of the driver while being properly positioned in the kart. The envelope validates that the driver can reach out for all control and emergency systems in dynamic and emergency conditions such as steering wheel, gear shifter, kill switch, fire extinguisher etc.

4. Steering

(a) Design Methodology

The methodology according to which steering system is designed is: it should have high sensitivity, directional stability, low minimum turning radius, desired steering ratios and the most important, it should follow Ackermann geometry to reduce tire wear. During turning if I-centers of all wheels meet at a point, then the vehicle will take turn about that point which results in pure rolling of the vehicle. The condition is called the Ackermann condition and this principle is known as Ackermann principle [17].
To select suitable steering system for the Go-Kart, 2 types of steering systems i.e Pitman Arm steering and Rack and Pinion arrangement have been studied. Amongst these, we chose Pitman Arm arrangement over the rack and pinion arrangement to its simplicity and low cost. Different properties of these two steering systems is shown in Table 13.

Table 13 : Pitman Steering VS Rack and Pinion Steering

Pitman Steering	Rack and Pinion
Simple 4 bar arrangement	Complex
Provides stiffness	Excessive free-play
Easy to fabricate	Difficult to fabricate/construct
Low cost of manufacturing	High cost of manufacturing
High chances of failure for long use of triangular plate	Less chances of failure for long use of rack and pinion gear

(b) Geometry Specifications

An optimum steering geometry was determined keeping in mind the desired steering ratio required for excellent vehicle control and following the Ackermann principle to the highest degree.
Factors keeping in mind for steering geometry design-

- Assumed values considering ergonomics and IKC rulebook.
- Wheel base- 1100mm
- Track width-880mm (80% of wheel base)
- Kingpin pivot to kingpin pivot point – 700mm.
- Minimizing turning radius
- Ackerman deviation for less range.

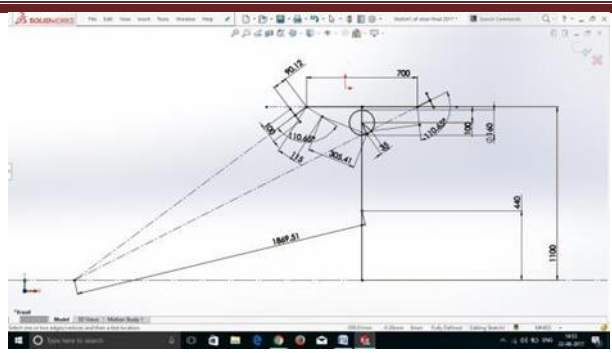

Fig. 19 (a) 2D sketch of steering linkage

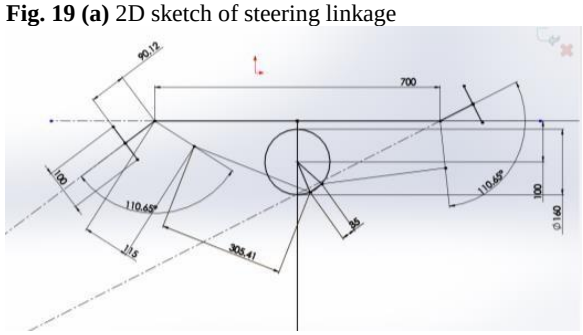

Fig. 19 (b) 2D sketch of steering linkage

Fig. 19 (a) and Fig. 19 (b) shows a 2D sketch of steering linkage which is made with the help of SolidWorks 2016. Fig. 20 shows the CAD model of steering system

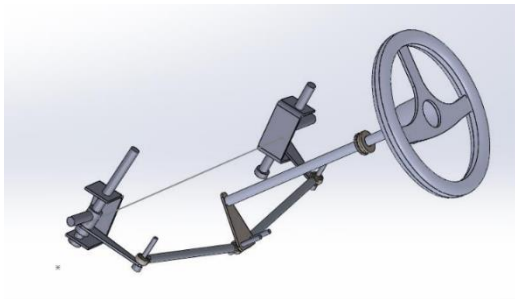

Fig. 20 : CAD model of Steering system

Table 14 : Values of Different Steering Parameters

Wheelbase	1100 mm
Track width	880 mm
Steering wheel diameter	304.8 mm (12
Spindle to spindle distance	700 mm
Length of steering arm	115 mm
Steering arm angle	17.65 deg
The rod length	305.41 mm
Maximum steering wheel angle	38.78 degree
Deviation of inner wheel at Ackermann	36.85 degree
Deviation of outer wheel at Ackermann	26.03 degree

(c) Turning Radius

The minimum turning radius of kart, as calculated came to be about 1.89m but due to deviation from Ackermann principle it will be locked at 1.79m so steering stops needed at position where turning radius is 1.89m to avoid over or under steering effect and wear and tear of tires.

(d) Steering Ratio

For providing a proper control over the kart, the steering ratio was kept nearer to 1:1 since it helps in good handling at high speeds and a better sense of control for the driver while maintaining high sensitivity for a faster response during turning.
Curve was generated with model in MSCAdams shown in figure 21.

e) Calculated Results

1. Steering Effort = 110-120 N (115.95 N at static condition)
2. Ackermann percentage = 105.3% (The values of Ackermann percentage come out to be greater than 100% which means the kart will have a tendency to oversteer).

3. Steering ratio= 1:1

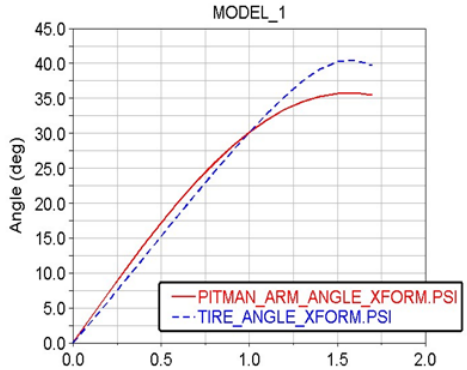

Fig. 21 : Comparison between steering angle and tyre angle

(e) Calculated Results

1. Steering Effort = 110-120 N (115.95 N at static condition)
2. Ackermann percentage = 105.3% (The values of Ackermann percentage come out to be greater than 100% which means the kart will have a tendency to oversteer).
3. Steering ratio= 1:1

(f) CAE on Steering

The following stress and strain simulations have been done using ANSYSv12. It accounts for the deformation under applied stress for the member used on the front wheels connected to chassis with fixed and knuckle and ultimately to the tires of the kart.

(i) Knuckle Mount Simulations

The following simulations were done on the ANSYS V12 which accounts for the deformation under the applied force of about 320 N approximately.

On the basis of load applied the following results have been obtained. Different iterations for different materials has been performed out of the iterations, mild steel hardened suits best.

Fig. 22 (a) : Kingpin mounting

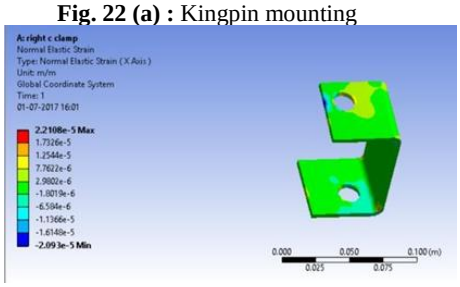

Fig. 22 (b) : Normal Elastic Strain Developed

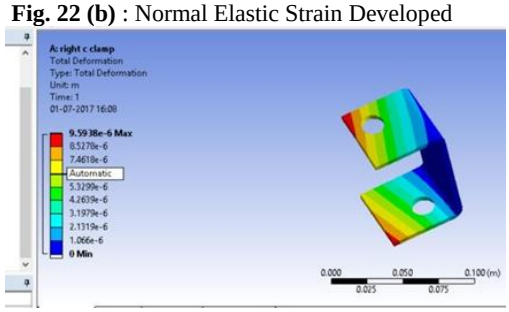

Fig. 22 (c) : Total Deformation under the Applied Stress

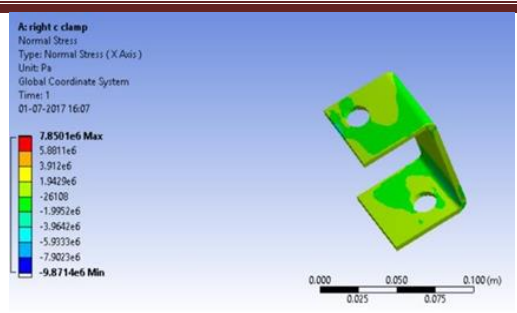

Fig. 22 (d) : Normal Stresses Developed

(ii) Knuckle Simulations

The following simulations have been done on the ANSYSv12 which accounts for the deformation under the applied force of 320 N approx. On the basis of load applied the following results have been obtained. For knuckle EN9 suits best as it has high weldability low hardness and is easily available.

Table 15 : Material Properties [7]

Materials	**EN8**	**EN9**	**EN 24**	**Plain Carbon Steel**
Density	7.8	7.8	8.17	7.8
Yield Strength(MPa)	465	480	680	220.6
Hardness (HRC)	51	48	55-65	38-40
Machinability	Very Good	Best	Worse	Good

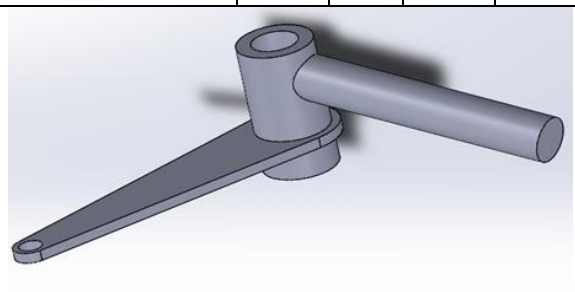

Fig. 23 (a) : CAD model of Steering Knuckle

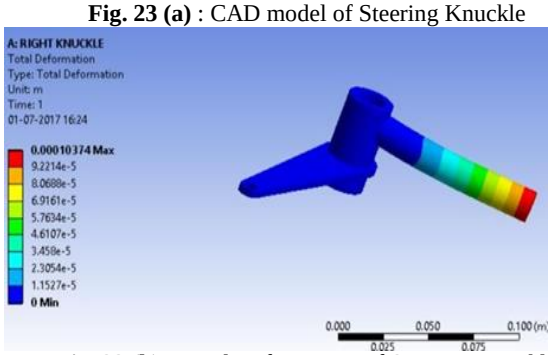

Fig. 23 (b) : Total Deformation of Steering Knuckle

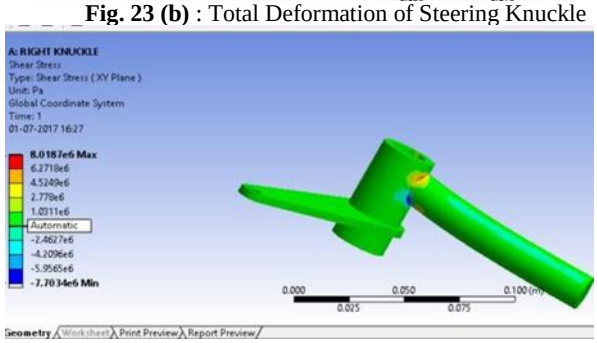

Fig. 23 (c) : Shear Stress in Steering Knuckle

Fig. 23 (a) shows the CAD model of steering knuckle.

Fig. 23 (b) shows the total deformation in the steering knuckle under the applied load or stress.

Fig. 23 (c) shows the distribution of the shear stress induced in the knuckle.

(g) Wheel Alignment Selection

Castor: We will provide positive caster angle of 10 degrees, since it will be helpful in proper weight transfer of the kart and the driver to the rear outer wheel of the kart during a turn which significantly reduces the weight on the inner rear wheel.

Camber: We provided zero camber angle because providing camber in go-kart will increase the wire wear during straight lines movement. Providing a caster angle also helps in giving a favorable automatic camber effect to the kart.

Toe: We gave toe of 3 degrees of angle for reducing turning radius and in dynamic condition tyres tend to toe out due to scrub radius so toe is compensated. It also helps in straight line stability with cornering compromised a little.

Kingpin axis inclination: We have provided 10 degrees, since it decreases scrub radius and induce jacking of rear inner tyre while turning at high speed.

5. Engine and Transmission

(a) Engine

For selecting the engine for our project, the following factors were considered in the listed order of priority:

- High Initial Torque
- High Torque at corner exits
- Cost
- Availability
- Power by weight ratio
- High power

Based on these factors, it was concluded that a manual transmission drive is essential for obtaining the desired performance characteristic curves. Further, the limitation on size of the engine confines the available choices of engines. The models of vehicle engines studied on the basis of the above mentioned criteria were: By considering factors such as maximum power, torque delivered by the engine, we have chosen the Honda Stunner engine for our go kart. The engine is heavier and more expensive than the Bajaj Discover engine, but this factor has been compromised due to the fact that Honda stunner engine is mounted vertically straight unlike the Bajaj Discover engine, which reduces our wheel base, thus making our chassis more compact.

Table 16 : Engine Specifications [8]

Displacement	124.7cc
Type of Fuel	Petrol (Spark Ignition)
Number of Strokes	4
Type of Cooling	Air cooled
Maximum Power	11.6 bhp @ 8000 rpm
Maximum Torque	11 Nm @ 6250 rpm
Air Filter	Viscous type
Bore of Engine	52.4 mm
Stroke of Engine	57.8mm
Compression Ratio	9.2:1
Clearence Volume	15.2073cc
Volumetric Efficiency	0.85
Mileage	60kmpl

(b) Engine Mounting

Engine mounting is a very crucial point that is needed to be taken care of. Proper mounting of the engine prevents the engine from possible damage as well it damps the engine vibrations.

The engine is bolted to the space frame chassis using high strength nut-bolts and washers at three points.

(c) Engine Support Base

The 28.64 Kg 124.7cc Honda CBF Stunner engine is mounted on a U-shaped member placed on a flat metal plate with 6mm. This support member is made from AISI 1020 steel and the failure while minimizing the weight. FEA simulation using Ansys of the support are carried out in order to check if the used system will perform adequately or not.

Static analysis result of the ANSYS Static Structural solver is shown. The analysis showed that the maximum stress within this member is 16.414 MP which is way beyond the yield strength of the AISI 1020 material, hence there are no chances of member failure during a race. The modal analysis results are shown in Fig. 25. As we know that the maximum speed of the engine is 10000 RPM which gives a primary imbalance frequency of 166.66 Hz and secondary imbalance of 333.33Hz. The modal analysis shows that the smallest natural frequency of the base member is 921.3Hz which is larger than the engine's frequency.

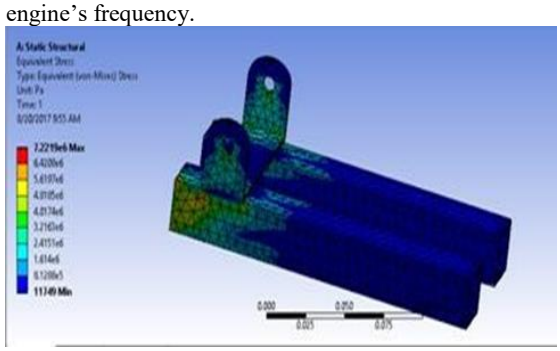

Fig. 24 : Equivalent Stress on Engine Support Base

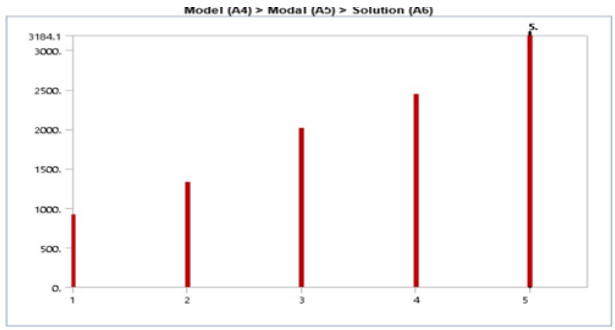

Model (A4) > Modal (A5) > Solution (A6)

Mode	Frequency [Hz]
1.	921.83
2.	1331.5
3.	2011.6
4.	2443.4
5.	3184.1

Fig. 25 : Modal Analysis

(d) Fuel Tank

Fuel tank is mounted just above the engine slightly backwards and sufficient space is provided between engine and fuel tank. The fuel tank is bolted to the chassis, which has a capacity of 5 litres.

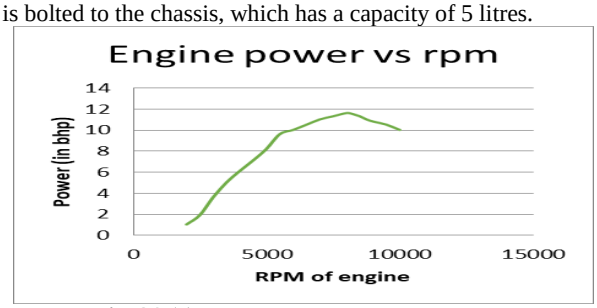

Fig. 26 (a) : Engine Power vs RPM

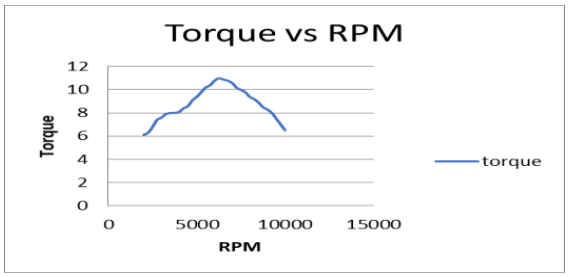

Fig. 26 (b) : Torque vs RPM
Fig. 26 : Engine Performance Curves

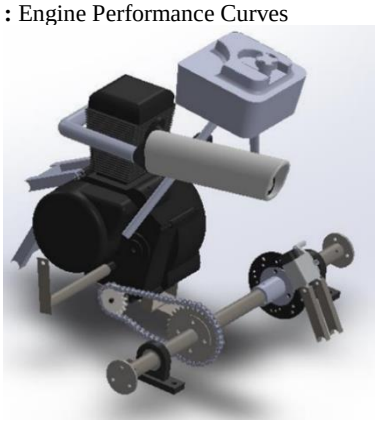

Fig. 27 : Engine CAD Model and Transmission Assembly
CAD model of the engine and transmission of the kart made using Solidworks.

(e) Transmission

A transmission is a machine that consists of a power source and a power transmission system, which provides controlled application of the power. Often the term transmission refers simply to the gearbox that uses gears and gear trains to provide speed and torque conversions from a rotating power source to another device. Often, a transmission has multiple gear ratios with the ability to switch between them as speed varies [18].

Honda CBF Stunner 125cc engine is accompanied by a five speed sequential gearbox with the following gear ratios.

Table 17 : Gear Ratios [8]

Primary Reduction Ratio	3.35
1st gear	3.076:1
2nd gear	1.944:1
3rd gear	1.473:1
4th gear	1.19:1
5th gear	1.038:1
Secondary or Final Reduction Ratio	3.071:1

For secondary reduction:
No. Of teeth on driver sprocket =14
No. Of teeth on driven sprocket =43
Calculation of maximum speed of bike:
Max Speed = r * ω
r = radius of rear tyre; ω = angular velocity of rear wheel
Aspect ratio is= 90 % and the width of tyre is 100mm.
Therefore, height of tyre= (90*100) / 100 = 90mm
Radius of Tyre (r) = (Rim Diameter * 0.5) + Tyre Height
= 309.5mm = 0.3095m. (Rim Diameter = 17 inches)
Angular velocity Maximum (ω)

$$= \frac{Max\ Engine\ RPM * 2\pi}{Primary\ Reduction * 5th\ gear\ ratio * secondary\ reduction * 60}$$

= (10000*2π) / (3.35*3.071*1.038*60)
= 98.063 rad/s.
Speed = 0.3095 * 98.063 = 30.35 m/s
= 109.26 km/hr

We made an indirect approach to calculate the appropriate size of the sprocket for limiting the maximum speed of the go-kart to 70 kmph (19.44m/s), by using the max. speed of the Honda stunner.
Max. Speed of the Honda stunner= 109.26 kmph = 30.35 m/s
∴ Max. RPM of the bike wheel (rear)= 936.41 rad/s.
∴ Max. RPM of secondary reduction driver sprocket
= Max wheel rpm * secondary reduction = 936.41 * 3.071 = 3003.1558 rad/s.
Also, RPM of the go-kart wheel at the Max Speed.

$$\frac{\max speed * 60}{2\pi * radius\ of\ wheel} = \frac{19.44 * 60}{2\pi * 0.1397} = 1328.83 \text{ rpm}$$

Required sprocket ratio (secondary reduction) * RPM of the go-kart wheel= 3003.155 rad/s. Required sprocket ratio = 3003.155/1328.83 = 2.26
No. of teeth on the required sprocket = 2.26*14 = 31.64 ≈ 32 (No. of teeth has to be a whole number).
Hence, we choose a sprocket ratio of 2.26, because it will serve both the purpose of giving high initial acceleration and limit the top speed to 70 kmph.
Coefficient of friction = 0.85 (For dry slick tyres)
Max force due to friction = Vertical force on wheels*coefficient of friction = (104*9.8)*0.85 = 866.32N
Maximum frictional torque on the rear wheels = Force on rear wheels * radius of rear wheel= 866.32*0.1397 = 121.024 Nm
866.32 N is the maximum external force available to the rear wheels for driving the kart.

Table 18 : Maximum theoretical speed for each gear at maximum RPM

Gear	Maximum Velocity
1st gear	6.28m/s = 22.60 kmph
2nd gear	9.939m/s = 35.78 kmph
3rd gear	13.11m/s = 47.196kmph
4th gear	16.23m/s = 58.42kmph
5th gear	19.44m/s = 70kmph

5.1 Sprocket Calculations in Accordance With Race Track

Fig. 28 : Mohite Racing Academy [23]
We decided to make a sprocket on the basis of a proper standard racing track by using Google maps we took out the maximum length of the track and scaled it with the scale available from the map and designed the kart's maximum velocity in accordance with it. The length came out be 160 meters.
We take the minimum turning radius to be 6 meters we found out the maximum velocity of the kart at which it could turn without skidding.
Velocity = $\sqrt{\mu * r * g}$ = $\sqrt{}$ .85*6*9.8 = 7.06 m/s = 25.45 kmph.
When the kart reaches the end of the other end of the longer part of the track, it needs to slow down and after calculation of the breaking force it is determined that 30 m of distance will be required to bring the kart to 25 kmph for making the other turn. Now the kart has 130 metres distance for it to reach the top speed maintain it for a certain distance and then again slow down.
Lets calculate the acceleration due to the rolling resistance.
Rolling Resistance = Fr = (0.02) * (160 kg) * (9.81 m/s^2)
= 31.392 Newtons
Kart acceleration due to rolling resistance
= - (31.392/160)= - 0.1962 m/s^2.
→Maximum acceleration in 3rd gear =

$$\frac{\text{Max. engine torque} * \text{primary red} * \text{Secondary Red} * \text{3rd gear ratio}}{\text{Wheel radius} * \text{mass of kart}}$$
$= \frac{11*3.35*2.26*1.473}{0.1397*60} = 5.3$ m/s^2.

Maximum acceleration in 3rd gear after consideration of rolling resistive force = 5.3 – 0.1962 = 5.1038 m/s^2.

Distance travelled till max speed is achieved in 3rd gear

Let us consider that it takes 1 sec for the gear shift to take place. Now during this time the force acting on the kart will be due to rolling resistance.

Hence distance travelled

= (13.11*1) – (0.5)*(0.1962)*(1^2) = 13.0119 m

Speed at the end of 1 second

= 13.11 - (0.1962*1) = 12.9138 m/s

→Maximum acceleration in 4th gear =

$$\frac{Max.engine\ torque * primary\ redn * Secondary\ redn * 4th\ gear\ ratio}{Wheel\ radius * mass\ of\ kart}$$
$= \frac{11*3.35*2.26*1.19}{0.1397*160} = 4.4$ m/s^2

Maximum acceleration in 4th gear after consideration of rolling resistive force = 4.4 – 0.1962= 4.2038 m/s^2

Distance travelled till max speed is achieved in 4th gear

= (16.23^2 − 12.91^2) / (2∗4.2038) = 11.50 m

Let us consider that it takes 1 sec for the gear shift to take place. Now during this time the force acting on the kart will be due to rolling resistance.

Hence distance travelled = (16.23*1) – (0.5) * (0.1962) * (1^2)= 16.1319 m

Speed at the end of 1 second = 16.23 – (0.1962*1)= 16.0338 m/s

→ Maximum acceleration in 5th gear

$$= \frac{Max.\ engine\ torque * primary\ redn * secondary\ redn * 5th\ gear\ ratio}{Wheel\ ratio * mass\ of\ kart}$$
$= \frac{11*3.35*2.26*1.038}{0.1397*160} = 3.8$m/s^2

Maximum acceleration in 5th gear after consideration of rolling resistive force = 3.8 -0.1962 = 3.6038 m/s^2

Distance travelled till max speed is achieved in 5th gear

= (19.442 − 16.03382) / (2∗3.8)= 16.76 m

Total distance required

= (11.891+13.0119+11.50+16.1319+16.76)= 69.2948 m

This distance obtained is less than the actual distance required as we have in our calculations taken into consideration peak torque available from the engine at all time which is not possible. We still have 60 m of distance available with us to reach top speed and maintain it for some period of time.

Hence limiting the top speed of kart to 70 kmph is appropriate.

5.2 Maximum Accleration At Different Gears:

The maximum acceleration in the 3rd, 4th, 5th gears have been stated earlier. The acceleration in the 1st, 2nd gears will be decided by the maximum frictional force available to the wheels as in both the gears the max force generated by engine exceeds frictional force.

Max. Force in 1st gear = (11*3.35*3.071*2.26) / 0.1397

= 1830 N, which is greater than the force available due to friction.

Max. Force in 2nd gear = (11*3.35*2.26*1.944) / (0.1397) = 1158.9 N, which is greater than the force available due to friction.

Hence, we use the max. available frictional force for the calculation of acceleration for both 1st, 2nd gear.

Max Acceleration = (866.32/160) = 5.41 m/s^2

Max Acceleration after consideration of rolling resistance = 5.41 – 0.1962 = 5.2 m/s^2

Table 19 : Maximum acceleration at different gears

Gear	Maximum Acceleration
1st gear	5.2 m/s^2
2nd gear	5.2 m/s^2
3rd gear	5.1 m/s^2
4th gear	4.2 m/s^2
5th gear	3.6 m/s^2

5.3 Tractive Force Vs Kart Speed Graph:

The graph plotted is on the basis of maximum force that the can be extracted from the engine and the kart speed. The maximum limiting frictional force is not considered.

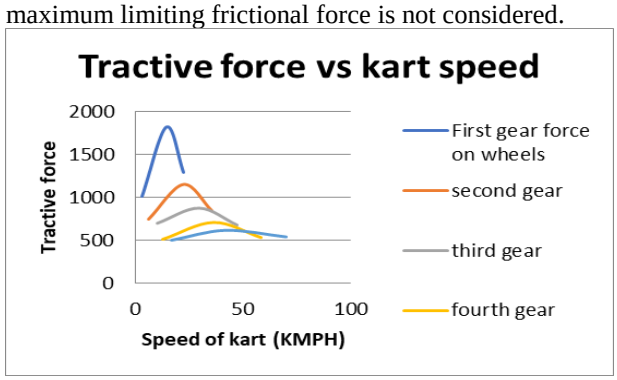

Fig. 29 : Tractive Force vs Kart Speed

5.4 Minimum Torque Required To Start The Vehicle

When we are just required to start the kart on a horizontal plane we just need to overcome the rolling resistance of the kart so we calculate the torque to overcome the rolling resistance of the kart.

Air resistance will not act as the kart is needed to just start from rest.

We take rolling resistance into account for the calculation of minimum torque.

Rolling Resistance = Fr

= (0.02) * (160 kg) * (9.81 m/s^2) = 31.392 N

This is the resistance offered when the vehicle is moving. For the starting of the kart this will be more.

We multiply the force by a factor of 2.5

Therefore, total force = 2.5 * 31.392 = 78.48N

Torque = 78.48 * 1397 = 10.9636 Nm

5.5 Transmission Efficiency

At lower gear ratios and relatively lower loads the transmission efficiency is assumed to be the following:

Transmission efficiency of a spur gear transmission = 97%.

Transmission efficiency of a chain and sprocket transmission = 98%. [11]

So, there is primary reduction using spur gears.

Another spur gear contact when there is transmission from input to output shaft. Final one is the chain and sprocket reduction.

Therefore, the total efficiency = 0.97 * 0.97 * 98 = 0.922 =92.2%

5.6 Power In Each Gear At Maximum Engine Torque:

Power = 2π*N*T/60*G

Here N = Engine rpm at maximum torque,

T = torque at the axle

(Max torque * Primary reduction * gear ratio * secondary reduction)

G= total gear reduction

(Primary reduction * gear ratio * secondary reduction)

N = Engine rpm corresponding to maximum torque.

$$\text{Therefore Power} = \frac{2\pi * n * \text{Max torque} * \text{primary redn} * \text{gear ratio} * \text{secondary redn}}{60 * \text{primary redn} * \text{gear ratio} * \text{secondary redn}}$$
$= \frac{2\pi * N * \text{Max torque}}{60} = 9.6$ hp= 9.6 * 746 = 7161W

Power at axle depends only upon the engine.

5.7 Rear Axle

We studied about various materials and then we concluded from it which material has to be chosen for the various things such as axle, hubs, and sprocket. We had analysed many materials on the basis of their properties, availability, and cost and then picked up the best one from amongst the choices available. Table 20 shows the details of the various materials that we studied.

Machinability comes out best for EN9, we are compromising the yield strength factor being maximum for EN24 for the sake of getting a lower hardness value to decrease the brittleness of the material. The hardness of EN9 is considered suitable, hence we choose EN9 as the material for our sprocket.

For hub selection, considering the above mentioned factors plus the weldability of the material, EN 9 can be welded much easily, hence we choose EN9 as the material for our hubs (Table 21).

AISI 1020 is chosen as the material for our axle as it is comparatively cheaper and readily available. It has lower yield strength as compared

to AISI 4130 and lower Machinability has been compromised with low cost of AISI 1020.

The outer diameter of the AISI 1020 is near to our requirement (35mm) comparative to other materials so that we can easily put our key into the axle. Moreover its bending stiffness is better than others and suits our requirements.

AISI 1020 is better than others due to its low cost, easy availability and high bending stiffness which is suitable for our engine mounting material.

Table 20 : Comparison of shaft materials [7]

Table 21 : Comparison of sprocket and hub materials [7]

Material	AISI - 1020	AISI - 4130	AISI - 4140	AISI - 1018
Density (g/cc)	7.87	7.85	7.85	7.87
Yield Stress (MPa)	350	460	415	370
Ultimate Stress (MPa)	420	670	655	440
Bending Stiffness (SI)	6150	3382.5	3408.4	5947.05
Outer Diameter of Axle (mm)	34.86	33.6	34.1	34.8
Thickness (mm)	3.21	2.743	2.77	3.17
Plummer Block Inner Diameter (mm)	32.1	27.486	27.7	31.64
Machinability (wrt AISI - 1212)	65 %	70 %	65 %	70 %

Materials	EN8	EN9	EN24	Plain Carbon Steel
Density	7.8	7.8	8.17	7.8
Yield Strength (MPa)	465	480	680	220.6
Hardness (HRC)	51	48	55-65	38-40
Machinability	Very Good	Best	Worse	Good

For Hubs of sprocket and wheel:

We chose Aluminium for the manufacturing of sprocket and the wheel hubs for the following properties it has:

- Light Weight (Density 2.7 g/cc)
- High Yield Strength
- Excellent Machinability
- Is easily weldable

Table 22 : Parameters used in calculation of loads

Property	Symbo	Value
Max. allowable shear stress	τ	30% of elastic limit =0.3*350=105MPa
Inner to outer diameter ratio	K	0.7
Radius of tire	R_T	0.1397 m
Distance b/w wheel & bearing	D	125 mm
Distance b/w sprocket & bearing (max.)	L_B	380 mm
Sprocket ratio	R_S	2.26
Outer Diameter of axle	D_o	-
Inner diameter of axle	D_i	-

When the kart is in motion, various bending and torsional forces act on axle, that is:

1. Bending moment due to the weight of the kart
2. Bending & twisting moment due to the engine torque
3. Twisting moment due to the Braking torque
4. Bending moment due to the braking force developed
5. Equivalent bending and twisting moment due to the combined effect of torsional and shear forces.

The maximum shear stress/normal stress theory is used to calculate the O.D. of the rear axle, which is subjected to the above described moments and torques and a combination of them.

5.8 Maximum Calculated Dynamic Weight Shift On The Rear Axle:

Weight shift due to the kart acceleration.

$W_r = W_{rs} + (W*H*a)/Lg$ [20]

Here W_{rs} = Weight on the rear wheels in the static condition.

H = Height of C.O.G from the ground (in mm)

L = Wheelbase of kart (in mm)

a = Maximum acceleration

$W_r = 104 + (160*5.2*200) / (1100*9.8) = 115.54$ kg.

Weight shift due to the gradient in the track.

$W_r = W_{rs} + (W*H*\sin\Theta)/L$ [20]

Max track gradient is assumed to be 4m rise in height for 100m run.

Therefore $\sin\theta = 4/100.7 = 0.0399$

$W_r = 104 + (160*200*0.399)/1100 = 105.16$ kg

Maximum weight on rear wheels = (104+15.4+.346) = 120.56 kg

Therefore, maximum force on rear wheels = 1037.4868 N

Common Constants Used: Calculation of the force that causes the bending in the axle:

calculate no of teeth in contact with the chain using the geometry of the sprockets. We can calculate the force shared by each teeth.

The no of teeth came out to be 21.

Now force will act tangentially on each of the sprocket teeth. We need to calculate the resultant of the forces.

The angle at which the forces act is calculated and then we add them vectorially.

Now the net resultant of these forces will cause the bending moment to take place.

Total force = (Total torque at shaft / Sprocket radius) = 255.75/.0645 = 3965.11 N

Force on each teeth acting tangentially to sprocket= (3965.11/21) = 188.80 N

Now the net resultant of these forces is calculated. Angles are calculated using Solidworks.

Therefore, the net resultant of the forces is =1783.2 N

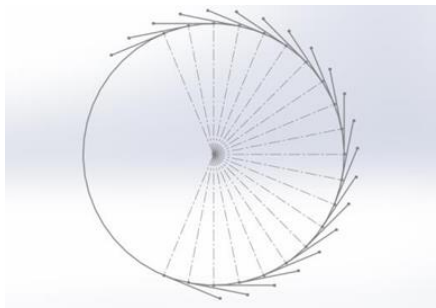

Fig. 30 : Force shared by each teeth

Table 23 : Formulae used in calculation of loads

Type of Loading (max. values)	Formula	Calculated
Bending moment due to the weight of the kart	MW = (reaction at wheels*distance between wheel and bearing)	64.75 Nm
Twisting moment due to the engine torque	TE = engine torque*final max. gear ratio	255.75 Nm
Bending moment due to the engine torque	ME = (bending force*max. dist. b/w sprocket & bearing)	677 Nm
Twisting moment due to the Braking torque (in case of hard braking)	TB = (reaction at one wheels*friction coefficient*wheel radius)	49.83 Nm
Bending moment due to the engine torque	MB= (Friction force on one wheel*distance between wheel and bearing)	44.59 Nm

5.9 Outer Diameter Calculations For Different Loading Conditions.

5.9.1 Type of Loadings

(a) Twisting of axle under the action of bending moment due to weight and engine torque and torsion caused by the engine.

$$D_o = \sqrt[3]{\frac{16\sqrt{[M_W+M_E]^2+T_E^2}}{\pi\tau(1-k^4)}} = 34.86 \text{ mm. [9]}$$

(b) Twisting of axle under the action of bending braking moment due to weight + force on wheels and torsion caused by braking torque.

$$D_o = \sqrt[3]{\frac{16\sqrt{[M_w+M_B]^2+T_B^2}}{\pi\tau(1-k^4)}} = 19.72 \text{ mm. [9]}$$

We have an axle available of material 35mm outer diameter and 25 mm inner diameter.

So we choose this one as one as the axle material.

Here are the Ansys results of the 2 cases that we calculated.

5.9.2 Type of Loadings: Twisting of axle under the action of bending moment due to weight and engine torque and torsion caused by the engine.

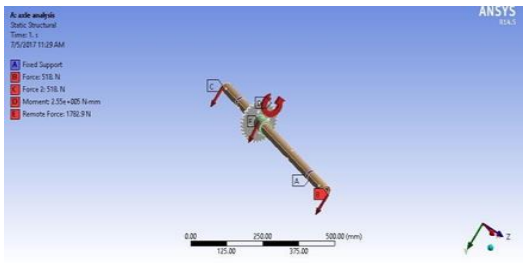

Fig. 31 (a) : Input of forces and moments

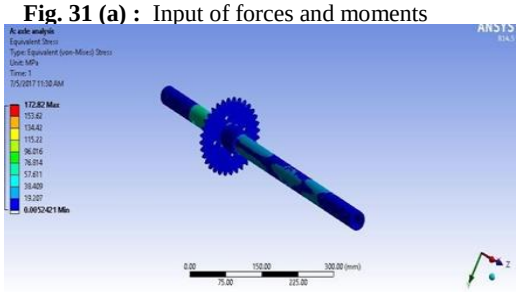

Fig. 31 (b) : Equivalent Stress

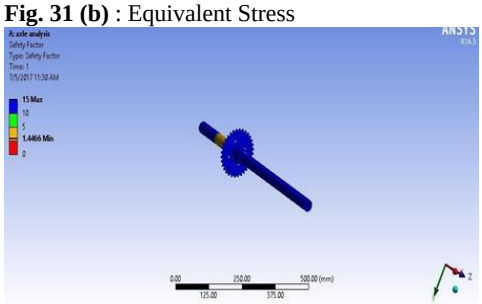

Fig 31 (c) : Factor of Safety

Fig. 31 : Type of Loadings

The equivalent stresses obtained in the axle are not exceeding the maximum value. The higher stresses that are present are induced in the key. Thus, we conclude that the axle shaft chosen is appropriate.

5.9.3 Type of Loadings: Twisting of axle under the action of bending braking moment due to weight + force on wheels & torsion caused by braking torque.

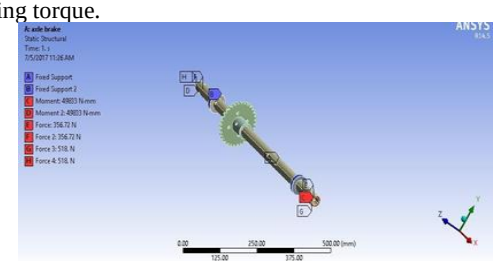

Fig. 32 (a) : Input of forces and moments

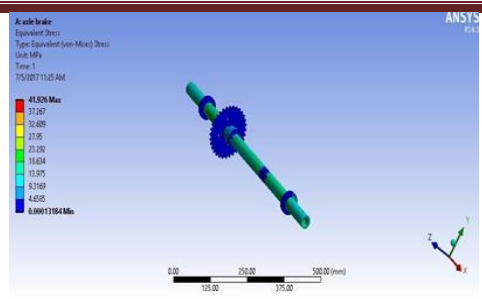

Fig. 32 (b) : Output of equivalent stresses

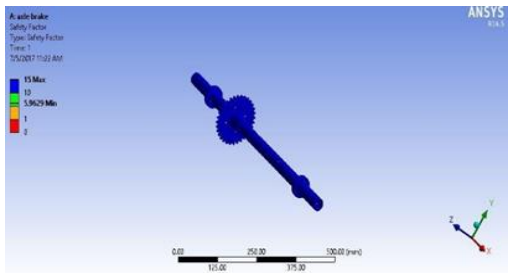

Fig. 32 (c) : Factor of safety

Fig. 32 : Type of Loadings

The stresses obtained in braking are way less than the maximum one which the axle can sustain during braking. Thus the axle will not fail.

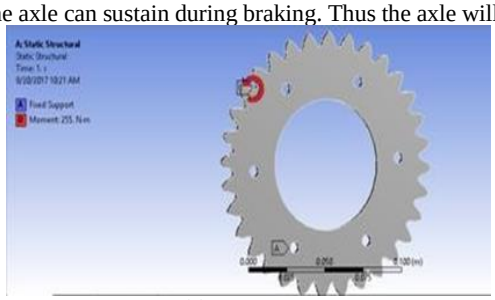

Fig. 33 (a) : Input of forces and moments

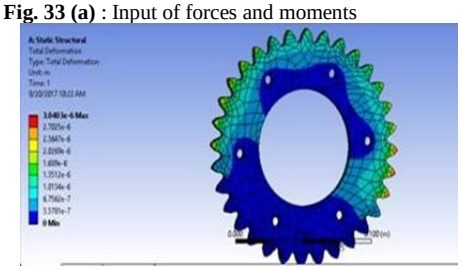

Fig. 33 (b) : Output of Equivalent Deformation

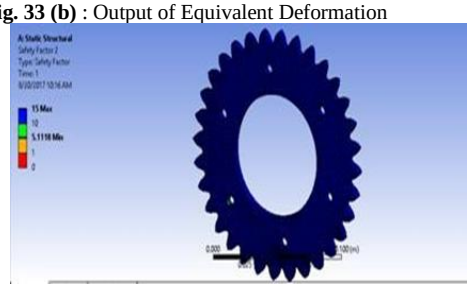

Fig. 33 (c) : Factor of safety

Fig. 33 : Analysis of Sprocket

In the case of sprocket the minimum factor of safety is 5, which is very high and hence sprocket will not fail

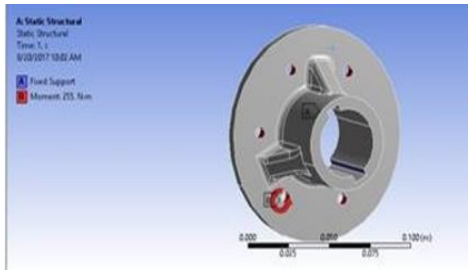

Fig. 34 (a) : Input of forces and moments

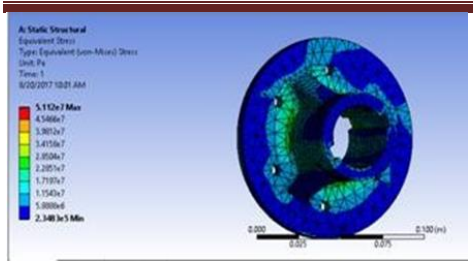

Fig. 34 (b) : Output of equivalent stresses

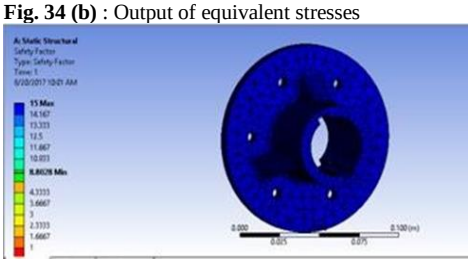

Fig. 34 (c) : Factor of safety

Fig. 34 : Analysis of Sprocket Hub

In the case of sprocket hub the max equivalent stress is just 51.253MPa, which is very low and hence sprocket hub will not fail.

6. BRAKES

6.1 Introduction

Brakes are an important mechanism on any vehicle because the safety of the driver depends on proper operation of the braking system. Brakes are an energy absorbing mechanism that convert the vehicle's kinetic energy into thermal energy, i.e. heat.

6.2 Objective

To design a braking system that can produce more than adequate braking force fulfilling IKC rules and regulations. The braking system should have following features:

1. The brakes must be strong enough to stop the vehicle within a minimum distance in an emergency.
2. The driver must have proper control over the vehicle during braking and vehicle must not skid.
3. The brakes must have well anti fade characteristics i.e. their effectiveness should not decrease with constant prolonged application.

6.3 Braking System Design

The brake system was designed according to the rules, restrictions, and requirements provided by the IKC rulebook. The Go-Kart has a hydraulic brake system which can be actuated by the brake pedal. DOT-4 has been chosen as the brake fluid. A comparison between drum brakes and disc brakes was done. Disc brakes were used in our vehicle due to these features-

1. Better stopping power.
2. Better heat dissipation due to increased effective area.
3. Drilled rotors enhance cooling whereas slotted rotors help in dirt removal.
4. Easy design, easy to inspect and completely self adjusting.

6.4 Brake Parts

The main parts used in the hydraulic braking system are –

1. Brake Pedal
2. Master Cylinder
3. Reservoir
4. Brake Hose
5. Brake Caliper
6. Brake Pads
7. Rotor

A single rotor was used on the rear axle of vehicle. Calculations were carried out for the condition of braking torque being greater than the frictional torque and it was observed that a single heavy caliper would be enough to stop the kart in a reasonable distance. A single master cylinder was used. The pedal was designed, analysed and manufactured by us.

Also, the rotor was manufactured after choosing the appropriate material, i.e. gray cast iron.

-Weight of the vehicle (W) = 160 kg -Max speed of vehicle (v) = 70 kmph = 19.44 m/s

-Radius of front tire(R_{front}) = 0.122m
-Radius of rear tire (R_{rear}) = 0.1397m
- Coefficient of Friction b/w road and tyre (μ) = 0.7
-Wheelbase (L) = 1.1m
-Horizontal distance from rear axle to C.O.G (X) = 0.405 m
-Vertical height of vehicle's C.O.G (h) = 0.1504 m
-Maximum deceleration(a) = 0.7g

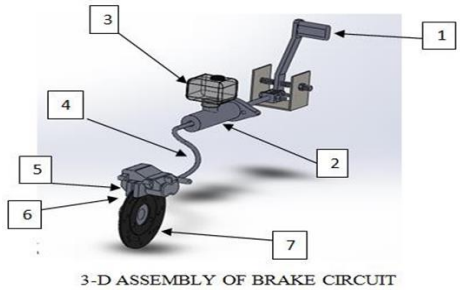

Fig. 35 : 3-D Assembly of Brake Circuit

6.5 Static Load Distribution On Axle [3]

Static load on rear axle = mg(L-X) / L = 990.7 N
Static load on front axle = mgX / L = 577.3 N
Distribution in static conditions is 63 : 37

6.5.1 Dynamic Load Transfer [3]

Dynamic load transfer of vehicle = mμgh / L = 150.07 N
Dynamic load on rear axle while braking (W_{rear}) = Static load on rear axle - Dynamic load transfer = 990.7 – 150.07 = 840.63
Dynamic load on front axle while braking (W_{front}) = Static load on front axle + Dynamic load transfer = 577.3+150.07 = 727.37 N
After braking, distribution is 53.5 : 46.5
Torque required to stop two rear wheels [3]=W_{rear} * μ * R_{rear} = 82.2 Nm
Frictional Torque at front wheels [3] = W_{front} * μ* R_{front} = 62.07 Nm

6.5.2 Braking System

Pedal effort = 200 N
Pedal Ratio = 6:1
Manual Pushrod Force (F_{mc}) = Pedal Effort * Pedal Ratio = 1200 N
Master Cylinder Bore = 19.05 mm
Area of MC Piston (A_{mc}) = 284.87 mm^2
Pressure in brake lines (P)= F_{mc} / A_{mc} = 4.212 MPa
Number of calipers = 1
Number of pistons in caliper = 2
Diameter of Caliper Piston = 25.4 mm
Area of Caliper Piston (A_{cal})= 506.45 mm^2
Force exerted by the caliper (F_{cal}) = P*A_{cal} = 4266.34 N
Coefficient of friction between pads and rotor = 0.3
Frictional force between pads and rotor (F_f)=0.3* 2 * F_{cal} = 2559.8 N
Effective rotor radius = 60mm
Braking Torque produced to stop the rotor= F_f * R_{eff} = 153.58 N
We can see that, Braking Torque > Frictional Torque
Rotor outer diameter = 170mm
Stopping Distance = $v^2 / 2a$
At v = 40kmph = 11.11 m/sec
For dry roads (μ = 0.7), stopping distance= 8.99 m
For wet roads (μ = 0.4), stopping distance= 15.74 m
Time to stop = v/a = 1.7 sec

Table 24 : Comparison of Disk Materials [7]

Grey Cast Iron (GCI)	Carbon Ceramic Composite (CCC)	Aluminum Composites (AC)
High Density Material	Moderate Density Material	Very Low Density Material
Moderate Specific Heat	High Specific Heat	High Specific Heat
Low Wear Rate	Very Low Wear Rate	Very High Wear Rate
Moderate Weight	Moderate Weight	Light Weight
Easily Available, Cheap to Manufacture	Expensive and Low Availability	Easily Available and Cheap

Preference of Materials is CCC > GCI > AC.
Although Carbon Ceramic composite had better properties, it was not chosen because of its high cost and low availability. Grey cast iron was chosen because of its easy availability, manufacturing and appropriate properties.

6.5.3 Pedal Effort Vs Deceleration

We have assumed a range of our driver's pedal effort from 100 N to 200 N. A graph between pedal force and corresponding deceleration has been plotted.
In braking conditions, force on rear wheels, = $F_f * R_{eff} / R_{rear}$
Deceleration = Force / W

Table 25 : Pedal effort vs Deceleration

Pedal Effort (N)	Deceleration(g units)
100	0.350
125	0.4375
150	0.525
175	0.6125
200	0.7

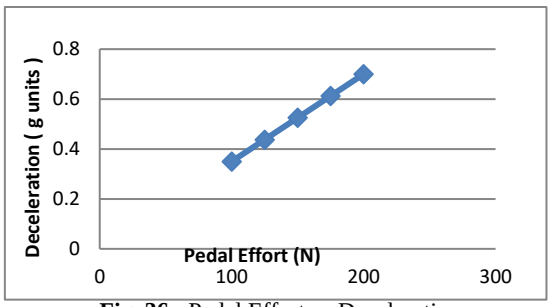

Fig. 36 : Pedal Effort vs Deceleration

6.6 Brake Fluids

A comparison of different types of fluids is given in table 26

Table 26 : Comparison of Brake Fluids [12]

DOT 3	DOT 4	DOT 5
Polyglycol Based-Glycol Ether	Polyglycol Based-Glycol Ether	Silicon Based
Amber Color	Amber Color	Purple Color
Absorbs moisture quickest	Lower absorbing power than DOT 3	Doesn't absorb moisture
Lowest boiling of °	Boiling Point- 2 °C	Highest Boiling Point
Restricted for road use only	High temperature tolerance	

DOT 4 brake fluid was used in the braking system because of the desired properties and its availability, low cost and eco friendliness.

6.7 Properties of Rotor and Pad Material

Material of Rotor - Grey Cast Iron
Material of Brake Pads - Mixture of semi-metallic and ceramic material.

Table 27 : Material properties of rotor and pad [7]

Material Properties	Pad	Disc
Thermal conductivity K (W/m-K)	56	47
Density (kg/m^3)	2400	7060
Elastic modulus (GPa)	2.76	124
Coefficient of friction	0.3	

6.7 CAE Reports of Braking System

The rotor and pedal were designed in Solidworks 2016 and their analysis was done on ANSYS for the calculated forces.

6.7.1 Rotor Analysis

Outer Diameter of Disc = 170mm Thickness = 3mm The following simulations have been done using ANSYS .

6.7.1Total Deformation : It accounts for the deformation under applied stress for the disc used on the rear axle of the kart.

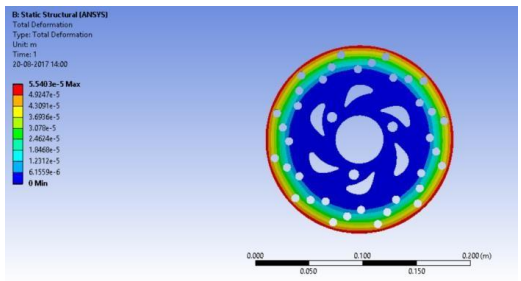

Fig. 37 (a) : Total Deformation

6.7.2 Thermal Analysis : It accounts for the distribution of temperature along rotor surface when it is stopped.

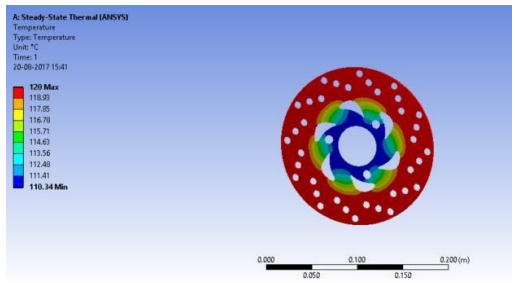

Fig. 37 (b) : Thermal Analysis
Fig. 37 : Rotor Analysis

6.7.3 Pedal Analysis

Pedal Ratio = 6:1.
The pedal effort ranges from 100N to 200 N, however, we tested our design for an application of maximum of 500N. The following simulations have been done on the pedal using ANSYS

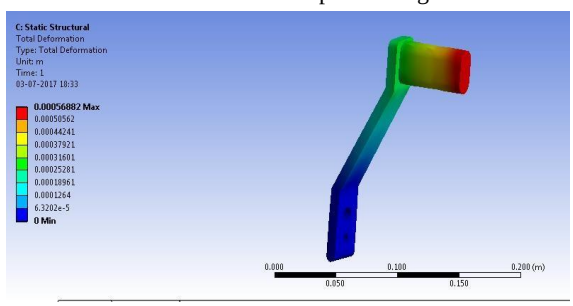

Fig. 38 (a) : Total Deformation

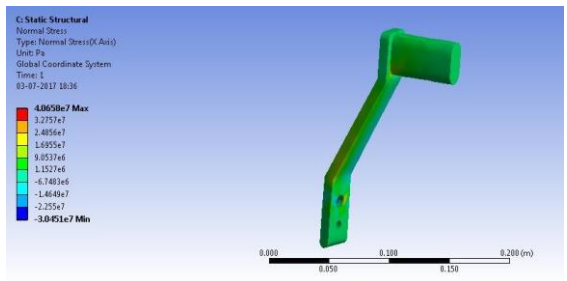

Fig. 38 (b) : Normal Stress

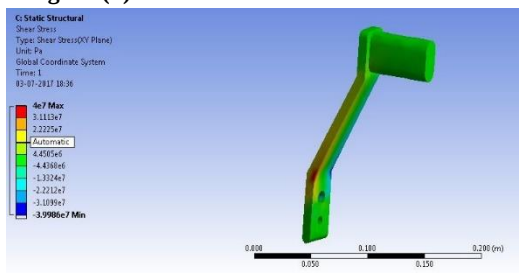

Fig. 38 (c) : Shear Stress
Fig. 38 : Pedal Analysis

Minimum factor of safety was found out to be 1.7 which approves our design.

6.8 Mounting Methods

The caliper mounting has been chosen such that bleeding point is at the top. Also, the brake rotor is attached to the axle with the help of a hub and keyway.

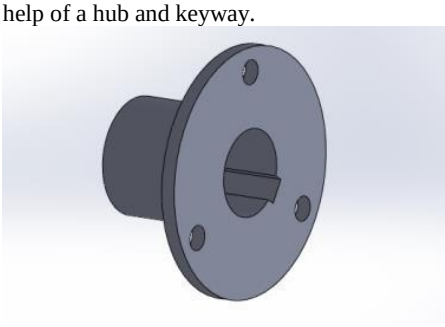

Fig. 39 : Hub and Keyway

6. Conclusions

The research paper has introduced new design concepts for the design of the Go-Kart chassis. The various in depth analysis performed on the design iterates and ensures that it meets the industrial safety standards. Focus has been laid on the new safety features that are feasible to implement and also monumental in an ever changing scientific landscape.

References

[1] K Parihar, N Negi, D Dimri, G Ramola, D Bhatt, S Gadal, N Singh, J Singh. Study and Examine the Go-kart Working Mechanism, International Journal of Scientific & Engineering Research, 8(12), 2017

[2] OC Zienkiewicz, RL Taylor. The Finite Element Method, Solid Mechanics, Fifth Edition.

[3] Limpert, Rudolf. Brake Design and Safety Society of Automotive Engineers, 1999 Second Edition.

[4] A Natu. Go-Kart Chassis Analysis: Design Methodology Integrating Revolutionary Safety Features, RAME Conference, ISBN: 987194523970-0

[5] KJ Wakeham. Introduction to Chassis Design, 1st edition, Memorial University of Newfoundland and Labrador, 2009.

[6] Indian Karting Championship (IKC) Rulebook, Season 4, 2018.

[7] www.azom.com, for material properties of all the components.

[8] https://bikeadvice.in/honda-cbf-stunner-125-review-sankesh/

[9] FP Beer, ER Johnston, JT Dewolf, DF Mazurek. Mechanics of Materials, Sixth Edition, ISBN: 978-0-07-338028-5.

[10] WF Milliken, DL Milliken. Race Car Vehicle Dynamics, ISBN: 978-1-56091-526-3.

[11] NPTEL: National Program on Technology and Enhanced Learning

[12] Ch7, Basic Hydraulic Systems- Peter Verdone Designs, 64-65, for the comparison of brake fluids.

[13] MH Mat, ARA Ghani. Design and Analysis of Eco Car Chassis, Procedia Engineering 41, 2012, 1756 – 1760.

[14] M Mahmoodi-k, I Davoodabadi, V Višnjić, A Afkar. Stress and Dynamic Analysis of Optimized Trailer Chassis, Technical Gazette 21(3), 2014, 599-608.

[15] R Rajappan, M Vivekanandhan. Static and Modal Analysis of Chassis by Using Fea, The International Journal of Engineering And Science (IJES), 2(2), 2013, 63-73.

[16] PA Renuke. Dynamic Analysis of A Car Chassis, International Journal of Engineering Research and Applications (IJERA), 2(6), 2012, 955-959

[17] D Koladia. Mathematical Model to Design Rack And Pinion Ackerman Steering Geomtery, International Journal of Scientific & Engineering Research, 5(9) 2014, 716-720.

[18] B George, A Jose, AJ George, A Augstine, AR Thomas. Innovative Design and Development of Transmission System for an Off-road Vehicle, International Journal of Scientific & Engineering Research (IJSER), 7(3), 2016.

[19] CR Prasad, MF Ahmed, MK Mohiuddin. Transmission System of Go-Kart, International Advanced Research Journal in Science, Engineering and Technology (IARJSET), 4(5), 2017 25-27.

[20] Gillespie, D Thomas. Fundamentals of Vehicle Dynamics, 1-14, ISBN: 978-1-56091-199-9, February 1992.

[21] G Mekalke. Static Analysis of a Go-Kart Chassis, International Journal of Mechanical and Industrial Technology, 3(2), 2015, 73-78

[22] A Singh, PK Jain, A Gupta. Design Analysis of the Chassis for the Go-Kart, V th International Symposium on Fusion of Science & Technology, New Delhi, India, January 18-22, 2016, ISBN: 978-93-84935-64-1

[23] Google Maps for race track satellite image.